Variations in the Influence of Diffuse Light on Gross Primary Productivity in Temperate Ecosystems

Susan J. Cheng[a,*], Gil Bohrer[b], Allison L. Steiner[c], David Y. Hollinger[d], Andrew Suyker[e], Richard P. Phillips[f], Knute J. Nadelhoffer[a]

[a]Department of Ecology and Evolutionary Biology, University of Michigan, Ann Arbor, MI 48109, USA

[b]Department of Civil, Environmental and Geodetic Engineering, The Ohio State University, Columbus, OH 43210, USA

[c]Department of Atmospheric, Oceanic and Space Sciences, University of Michigan, Ann Arbor, MI 48109, USA

[d]Northern Research Station, USDA Forest Service, Durham, NH 03824, USA

[e]School of Natural Resources, University of Nebraska-Lincoln, Lincoln, NE 68583, USA

[f]Department of Biology, Indiana University, Bloomington, IN 47405, USA

*Corresponding author: e-mail address: chengs@umich.edu, tel: +1 1734 647 3165

Abstract

The carbon storage potential of terrestrial ecosystems depends in part on how atmospheric conditions influence the type and amount of surface radiation available for photosynthesis. Diffuse light, resulting from interactions between incident solar radiation and atmospheric aerosols and clouds, has been postulated to increase carbon uptake in terrestrial ecosystems. However, the magnitude of the diffuse light effect is unclear because existing studies use different methods to derive above-canopy diffuse light conditions. We used site-based, above-canopy measurements of diffuse light and gross primary productivity (GPP) from ten temperate ecosystems (including mixed conifer forests, deciduous broadleaf forests, and croplands) to quantify the GPP variation explained by diffuse photosynthetically active radiation (PAR) and to calculate increases in GPP as a function of diffuse light. Our analyses show that diffuse PAR explained up to 41% of variation in GPP in croplands and up to 17% in forests, independent of direct light levels. Carbon enhancement rates in response to diffuse PAR (calculated after accounting for vapor pressure deficit and air temperature) were also higher in croplands (0.011-0.050 μmol CO_2 per μmol photons of diffuse PAR) than in forests (0.003-0.018 μmol CO_2 per μmol photons of diffuse PAR). The amount of variation in GPP and carbon enhancement rate both differed with solar zenith angle and across sites for the same plant functional type. At crop sites, diffuse PAR had the strongest influence and the largest carbon enhancement rate during early mornings and late afternoons when zenith angles were large, with greater enhancement in the afternoons. In forests, diffuse PAR had the strongest influence at small zenith angles, but the largest carbon enhancement rate at large zenith angles, with a trend in ecosystem-specific responses. These results highlight the influence of zenith angle and the

role of plant community composition in modifying diffuse light enhancement in terrestrial ecosystems, which will be important in scaling this effect from individual sites to the globe.

Keywords

Net ecosystem exchange; diffuse PAR; carbon cycling; land-atmosphere interactions

Highlights

- Impacts of diffuse light on gross primary productivity (GPP) were quantified.
- Diffuse PAR explains up to 17% (forests) and 41% (crops) of variation in GPP.
- The strength of the diffuse light effect varies with zenith angle and ecosystem.
- The largest increase in GPP occurs in maize croplands in the late afternoon.

1. Introduction

Forests are estimated to remove up to 27% of human-emitted CO_2 annually (2.6 ± 0.8 Gt C yr^{-1}), with temperate forests responsible for about half of this uptake globally (Le Quéré et al., 2013; Sarmiento et al., 2010). It is uncertain how this amount of carbon uptake will change in the future because forest carbon processes are affected by complex interactions driven by changes in climate and natural- and human-caused shifts in plant species composition and canopy structure. Isolating and quantifying the impacts of individual drivers of land-atmosphere CO_2 exchange could improve these calculations of the future terrestrial carbon sink.

One important factor influencing photosynthesis and hence forest CO_2 uptake is light availability. Rates of leaf-level CO_2 uptake increase with solar radiation until leaves are light saturated (Mercado et al., 2009). This implies that forest CO_2 uptake is greater on sunny days when leaves are fully exposed to direct light. However, increases in diffuse light, which is produced when clouds and aerosols interact with and scatter incoming solar radiation, may be even more beneficial than equal increases in direct light. At the ecosystem level, key processes related to photosynthesis, including gross primary productivity (GPP), net ecosystem exchange (NEE), and light-use efficiency (LUE), can increase in magnitude when the proportion of light entering a forest canopy is more diffuse (Gu et al., 1999b; Hollinger et al., 1994; Jenkins et al., 2007; Oliphant et al., 2011; Urban et al., 2012; Zhang et al., 2011). In addition, global simulations from 1960-1999 indicate that increases in the proportion of diffuse light reaching plant canopy surfaces may have amplified the global land carbon sink by 24% (Mercado et al., 2009).

Several mechanisms have been proposed to explain how diffuse light increases ecosystem CO_2 uptake and LUE. First, diffuse light can penetrate deeper into a forest canopy

72 and reach lower canopy leaves that would normally be light-limited on clear days when light is
73 mostly direct (Hollinger et al., 1994; Oliphant et al., 2011). Second, the same amount of light is
74 distributed across more leaves when diffuse light is dominant, which can minimize light
75 saturation and photo-inhibition of upper canopy leaves and increase canopy LUE or
76 photosynthesis (Gu et al., 2002; Knohl and Baldocchi, 2008). Third, diffuse light can create
77 conditions favorable for photosynthesis by reducing water and heat stress on plants (Steiner and
78 Chameides, 2005; Urban et al., 2012). Finally, a fourth hypothesis suggests that diffuse light has
79 a higher ratio of blue to red light, which may stimulate photochemical reactions and stomatal
80 opening (Urban et al., 2012).
81 There is no consensus regarding the magnitude of effect that diffuse light has on
82 ecosystem carbon processing. Studies using derived values of diffuse light suggest that LUE is
83 higher when most incident light is diffuse and can result in maximum carbon uptake under
84 moderate cloud cover (Gu et al., 2002; Min and Wang, 2008; Rocha et al., 2004). However,
85 studies using a three-dimensional canopy model and a land surface scheme predict that diffuse
86 radiation will not lead to significant increases in carbon uptake on cloudy days as compared to
87 clear days because of reductions in total shortwave radiation (Alton et al., 2005; Alton et al.,
88 2007). If clouds decrease surface radiation enough to lower total canopy photosynthetic activity,
89 this could offset any potential GPP gain resulting from increased LUE under diffuse light
90 conditions (Alton, 2008).
91 Several studies using measurements of diffuse light support the hypothesis that LUE is
92 higher under diffuse light, consistent with studies using derived diffuse light data (Dengel and
93 Grace, 2010; Jenkins et al., 2007). In addition, total carbon uptake can be greater under cloudy,
94 diffuse light conditions compared to clear skies in three forest types (Hollinger et al., 1994; Law

et al., 2002). Aerosol-produced diffuse light also leads to an increase in the magnitude of NEE in forests and croplands (Niyogi et al., 2004). Additional observation-based analyses indicate that diffuse light increases carbon uptake when compared to the same level of direct light, but also when total light levels decrease (Hollinger et al., 1994; Urban et al., 2007; Urban et al., 2012).

The magnitude of the diffuse light effect on terrestrial carbon uptake may depend on ecosystem type or canopy structural characteristics. A regional modeling study suggests that diffuse light can increase net primary productivity (NPP) in mixed and broadleaf forests, but has a negligible effect on croplands (Matsui et al., 2008). Another study using derived diffuse light data suggests that LUE increases with diffuse light, and that differences among ecosystems are potentially dependent on vegetation canopy structure (Zhang et al., 2011). The influences of ecosystem type and vegetation structure are also supported by an observation-based study showing that under diffuse light, CO_2 flux into a grassland decreased, but increased by different amounts in croplands depending on the species of crop planted (Niyogi et al., 2004). However, another study using derived diffuse light data found no difference in the effect of patchy clouds on LUE among 23 grassland, prairie, cropland, and forest ecosystems in the Southern Great Plains (Wang et al., 2008). Inconsistencies among these studies may be due to differences in the methods and models used to obtain diffuse light or sky conditions and assess their impacts on ecosystem carbon processing (Gu et al., 2003).

Climate modelers have begun incorporating the influence of diffuse light on ecosystem carbon uptake into land surface schemes as more details of canopy structure are added to models (Bonan et al., 2012; Dai et al., 2004; Davin and Seneviratne, 2012). Our study provides insight into the importance of diffuse light on ecosystem carbon processing for improving projections of

118 the terrestrial carbon sink. We seek here to 1) quantify how much variation in ecosystem GPP is
119 explained by diffuse light, independent of direct radiation levels, 2) compare the influence of
120 diffuse light on GPP among temperate ecosystems differing in canopy structure and species
121 composition, and 3) determine the strength of diffuse light enhancement of GPP while
122 accounting for its correlation with zenith angle, vapor pressure deficit (VPD), and air
123 temperature. Unlike many previous studies (Alton, 2008; Butt et al., 2010; Gu et al., 1999b; Min
124 and Wang, 2008; Zhang et al., 2010), we drive our analyses only with direct field measurements
125 of diffuse light, rather than with derived values from radiation partitioning models, which may be
126 biased by incorrect representations of clouds and aerosols. Finally, our paper highlights the
127 changes in the diffuse light effect across the diurnal cycle and the role of time of day on the
128 diffuse light enhancement in terrestrial ecosystems, which will be important in scaling this effect
129 from individual sites to the globe.

130 **2. Materials and Methods**

131 ***2.1 Data Sources***

132 All analyzed data were collected and processed by investigators participating in the
133 AmeriFlux program (http://ameriflux.lbl.gov/), a network of meteorological towers in the United
134 States (U.S.) that measures net fluxes of water vapor and CO_2 between the land surface and the
135 atmosphere and corresponding meteorological, soil, and vegetation conditions (Baldocchi, 2003).
136 Data collection, analysis, and metadata are standardized, reviewed, and quality controlled by
137 AmeriFlux for all sites. GPP is calculated by subtracting the modeled ecosystem respiration
138 from observed NEE. Respiration is modeled empirically based on NEE observations during the
139 night, when GPP is assumed to be zero. We focus our study on GPP instead of another measure
140 of carbon processing because it describes ecosystem CO_2 uptake, is affected directly by

141 radiation, and is the first step in processing atmospheric CO_2 into long-term storage in
142 ecosystems.

143 ***2.2 Site Selection***

144 We selected temperate AmeriFlux sites within the contiguous U.S. with at least three
145 years of Level 2 (processed and quality controlled) NEE and GPP. Among these, we specifically
146 selected sites that contain equipment to measure above-canopy total and diffuse
147 photosynthetically active radiation (PAR, 400-700 nm) and report at least three years of diffuse
148 PAR values to AmeriFlux. For the University of Michigan Biological Station (UMBS), we
149 obtained updated total and diffuse PAR data from site coordinators that were not yet available on
150 the AmeriFlux website at the time of our analyses. After separating sites with crop rotations by
151 species, there were sufficient data for ten sites covering three ecosystem types, including mixed
152 forest (Howland Logged, Howland N Fertilized, Howland Reference), deciduous broadleaf forest
153 (Morgan Monroe and UMBS), and cropland (Mead Irrigated Maize, Mead Irrigated Rotation:
154 Maize, Mead Irrigated Rotation: Soybean, Mead Rainfed Rotation: Maize, Mead Rainfed
155 Rotation: Soybean). Site characteristics and data availability are listed in Table 1.

Table 1: AmeriFlux site information and ecosystem characteristics

Site (SiteID)	Lat, Lon (°)	Years of Data	Canopy Height (m)	Vegetation Community	Management	LAI (m^2 m^{-2})	Climatic Annual Precipitation (mm)	Mean Growing Season Temperature[a] (°C)	Mean Growing Season VPD[a] (kPa)
Howland Logged (US-Ho3)	45.207, -68.725	2006-2008	20[b]	Dominated by red spruce (*Picea rubens*) and eastern hemlock (*Tsuga canadensis*). Also contains balsam fir (*Abies balsamea)*, white pine (*Pinus strobus)*, white cedar (*Thuja occidentalis*), red maple (*Acer rubrum*), and paper birch (*Betula papyrifera*)[c].	Selected logging and harvest (2001)[b]	2.1 to ~4[e]	1000[b]	16.7	0.83
Howland Reference (US-Ho1)	45.204, -68.740	2006-2008			Minimal disturbance since 1900s[d]	~ 6[b]		17.6	0.87
Howland N Fertilized (US-Ho2)	45.209, -68.747	2006-2009			N addition (2001-2005)[d,e]	~ 6[b]		16.5	0.82
Mead Irrigated Maize (US-Ne1)	41.165, -96.476	2001-2012	2.9[f]	Maize (*Zea mays)*	Center-pivot irrigation[f]	5.7[e]	887[f]	27.0	1.33
Mead Irrigated Rotation: Maize (US-Ne2)	41.164, -96.470	2001, 2003, 2005, 2007, 2009-2012	2.9[e]	Maize (*Z. mays)*	Center-pivot irrigation[f]	5.3[e]		26.2	1.14
Mead Irrigated Rotation: Soybean (US-Ne2)		2002, 2004, 2006, 2008	1.0[e]	Soybean (*Glycine max)*		4.9[e]			
Mead Rainfed Rotation: Maize (US-Ne3)	41.179, -96.439	2001, 2003, 2005, 2007, 2009, 2011	2.6[e]	Maize (*Z. mays)*	Naturally rainfed[g]	4.2[e]		26.7	1.39
Mead Rainfed Rotation: Soybean (US-Ne3)		2002, 2004, 2006, 2008, 2010, 2012	0.9[e]	Soybean (*G. max)*		3.8[e]			
Morgan Monroe (US-MMS)	39.323, -86.413	2007-2010	27[h]	Dominated by sugar maple (*A. saccharum*), tulip poplar (*Liriodendron tulipifera*), sassafras (*Sassafras albidum*), white oak (*Quercus alba*),	None	5[i]	1012[j]	24.3	1.12

				and black oak (*Q. nigra*)[h].					
UMBS (US-UMB)	45.559, -84.713	2007-2011	22[k]	Dominated by bigtooth aspen (*Populus grandidentata*) with red oak (*Q. rubra*), red maple (*A. rubrum*), and white pine (*P. strobus*), as co-dominants. Also contains trembling aspen (*P. tremuloides*), white birch (*B. papyrifera*), sugar maple (*A. saccharum*), red pine (*P. resinosa*), and American beech (*Fagus grandifolia*).[k]	None	~3.5[k]	817[k]	21.2	1.05

157 [a]Values calculated from AmeriFlux data, [b]Scott et al., 2004, [c]Hollinger et al., 2004, [d]AmeriFlux website, [e]personal communication
158 with site investigator, [f]Yan et al., 2012, [g]Verma et al., 2005, [h]Dragoni et al., 2011, [i]Oliphant et al., 2011, [j]Curtis et al., 2002, [k]Gough et
159 al., 2013

2.3 Definition of Analysis Period

To determine the maximum effect of diffuse light on GPP, we limited our period of analysis to the portion of the year when ecosystems are most productive. We used a carbon-flux phenology approach, where NEE is the defining variable for phenological transitions and the peak-growing season is the time period when NEE is at its maximum magnitude (Garrity et al., 2011). To do this, we first calculated 5-day NEE means for each site and year. Climate, vegetation composition, and inter-annual weather variability lead to phenological variation among sites (Richardson et al., 2013). Therefore, we adjusted our definition for the beginning and end of the peak-growing season to uniformly capture a representative portion of the NEE peak across sites and years. We defined the start of the growing season as the first day when the 5-day NEE average was within 90% of the year's fourth highest 5-day NEE average. The fourth-highest value was used to account for any extreme NEE values that may have occurred because of anomalous weather conditions. We set the end of season as the last day within 75% of the year's fourth-highest 5-day NEE average. The cutoff for the start of the peak-growing season is higher than the cutoff for the end of the season because canopy leaf-out and growth initiation typically occur quickly in seasonal sites, whereas canopy phenological changes are slower at the end of the season. While this approach cannot detect the exact beginning and end of the season, the criteria we used provide a uniform method for defining the period during which plants were at full seasonal growth and activity at our sites. We included only daytime values by excluding points with total PAR values < 20 μmol m^{-2} s^{-1}, assuming such low radiation levels are characteristic for nighttime.

2.4 Data Analysis

For each site, we combined all available peak-growing season daytime data and removed observations with negative measurements of diffuse PAR, direct PAR, or GPP, as these were likely sensor errors or marginal weather conditions (e.g., rain events). We also excluded data points with missing air temperature and VPD. We divided the remaining data into nine categorical groups based on solar zenith angle and the time of observation. We chose to bin by zenith angle to account for the effect of the sun's position on the amount of direct and diffuse PAR above a canopy, differences in radiation penetration through the canopy, and changes in plant hydraulics throughout the day. Zenith angle was calculated as the following:

$$\cos \varphi = \sin \phi \sin \delta + \cos \phi \cos \delta \cos [15(t - t_0)] \quad (1)$$

where φ is the zenith angle, ϕ is the latitude, δ is the solar declination angle, t is time, and t_0 is the time of solar noon (Campbell and Norman, 1998). Given the latitudes of the sites, we defined mornings to begin at zenith angles between 76-100°, noon to occur at the minimum calculated zenith angles of 16-30°, and the end of daylight to occur around 76-100°.

The effect of diffuse PAR on GPP may depend on total light conditions. For example, little scattering occurs under clear skies, which results in low diffuse and high direct PAR levels. As a result, small increases in diffuse PAR are unlikely to have a strong impact on canopy photosynthesis due to large amounts of direct PAR available for photosynthesis. If direct PAR levels are low, however, such as on cloudy days or during the morning and evening, the increase in diffuse PAR will have a larger effect because canopy leaves are below light-saturation. To calculate direct PAR, we subtracted the observed diffuse PAR from the observed total PAR. Because GPP and PAR are known to have a strong relationship that can be empirically described

by a rectangular hyperbola, we used the non-linear regression function in the R program (R Development Core Team, 2012) to fit the following relationship:

$$GPP_{fitted} = (\alpha\ \gamma\ PAR_{dir}) / (\gamma + \alpha\ PAR_{dir}) \quad (2)$$

where GPP_{fitted} is the value of GPP predicted by total PAR using a rectangular hyperbola model (Eq. 2), α is the canopy quantum efficiency, γ is the canopy photosynthetic potential, and PAR_{dir} is direct PAR (Gu et al., 2002). The α and γ are the fitted parameters and are solved iteratively. We used the initial conditions of 0.044 µmol CO_2 per µmol photons and 23.7 µmol CO_2 m^{-2} s^{-1} for α and γ, respectively (Ruimy et al., 1995). The resulting empirical relationships for each site are presented in Appendix 1.

To remove the confounding effect of direct PAR, we first calculated the residuals between observed GPP and GPP_{fitted}. We then compared those residuals against diffuse PAR for ten sites and nine zenith angle bins. For each zenith angle category, we estimated the variation in GPP residuals that can be explained by diffuse PAR alone using the following simple linear regression:

$$GPP_r = GPP - GPP_{fitted} = \beta_0 + \beta_1\ PAR_{diff} + \varepsilon \quad (3)$$

and a combination of diffuse PAR, VPD, and air temperature using the following multiple linear regression:

$$GPP_r = GPP - GPP_{fitted} = \beta_0 + \beta_1\ PAR_{diff} + \beta_2\ VPD + \beta_3\ T_a + \varepsilon \quad (4)$$

where GPP_r represents the residuals between the observed GPP and GPP_{fitted} and PAR_{diff} is diffuse PAR. T_a is air temperature measured at the eddy covariance tower and β_0, β_1, β_2 and β_3 are the fitted parameters estimating the model intercept and the linear slopes of the effects of diffuse PAR ,VPD, and air temperature at each solar zenith bin, respectively. The ε is the error term.

ANOVA comparisons between the simple (diffuse PAR only) and multiple linear regressions (including VPD and air temperature) showed that the multiple linear regression model (Eq. 4) was significantly better ($p < 0.05$) than the simple regression model, with the exception of nine site/bin combinations. We did not include interactions in the multiple linear regression because ANOVA tests indicated that the interaction terms did not improve the model consistently, and improvements to the residual sum of squares averaged only 3.5% in cases where interaction terms were significant. We also accounted for multiple testing over solar zenith angle bins and different sites by using the Bonferroni correction to calculate a new critical p-value. Light-response curves could not be fit to all scenarios, reducing the final number of comparisons to 83. Thus, for the simple and multiple linear regression comparisons, we consider a relationship significant if $p < 6.02 \times 10^{-4}$ (= 0.05/83).

3. Results

3.1 Relationship between diffuse PAR and GPP

We found significant positive relationships between diffuse PAR and GPP_r throughout the day, except in a few cases where diffuse PAR was not a significant predictor of GPP_r (Fig. 1, Fig. 2, black bars). Exceptions to these relationships occurred mainly at the Mead crop sites during mid-day and to a lesser extent at the UMBS forest during early mornings and late afternoons (Fig. 2, black bars). In addition, a rectangular hyperbola could not be fit to the direct PAR and GPP data in the afternoon at large zenith angles at the Mead sites and Morgan Monroe (Appendix 1). Overall, the linear fits between diffuse PAR and GPP_r indicate that across sites and zenith angles, diffuse PAR explains 3-22% of variation in GPP_r in the morning and 3-41% of variation in GPP_r in the afternoon (Fig. 2, black bars).

248 The amount of variance in GPP_r attributable to diffuse PAR varied considerably between
249 forests and crop sites (Fig. 2, black bars). At the deciduous broadleaf and mixed conifer forests,
250 diffuse PAR accounts for more of the variance in GPP_r at the smallest zenith angle bins (mid-
251 day) and less at larger zenith angles in the early mornings and late afternoons (Fig. 2a-e, black
252 bars). However, the opposite pattern occurs at the Mead crop sites, where more of the variance
253 in GPP_r is associated with diffuse PAR at larger zenith angles (Fig. 2f-j, black bars). Diffuse
254 PAR accounted for the largest portion of GPP_r variance at crop sites during afternoon zenith
255 angles of 61-75°, corresponding to approximately 17:00-18:00 standard time.

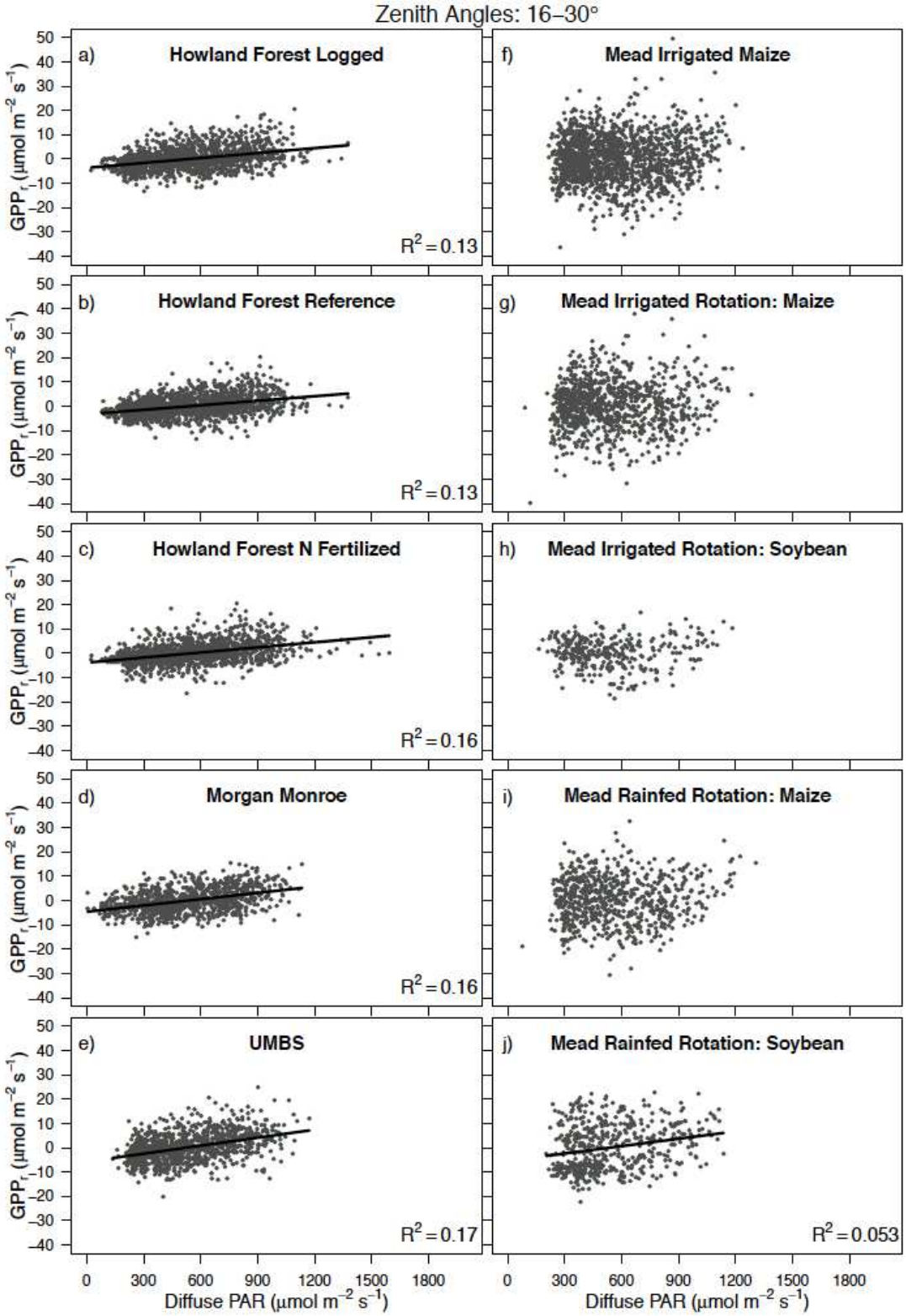

Fig 1. Simple linear regressions (Eq. 3) between diffuse PAR and GPP_r for observations around 10:00 – 14:00 standard time (zenith angles from 16-30°, other zenith angle bins not shown). Regression lines are only plotted for models with $p < 6.02 \times 10^{-4}$ (Bonferroni-corrected critical value).

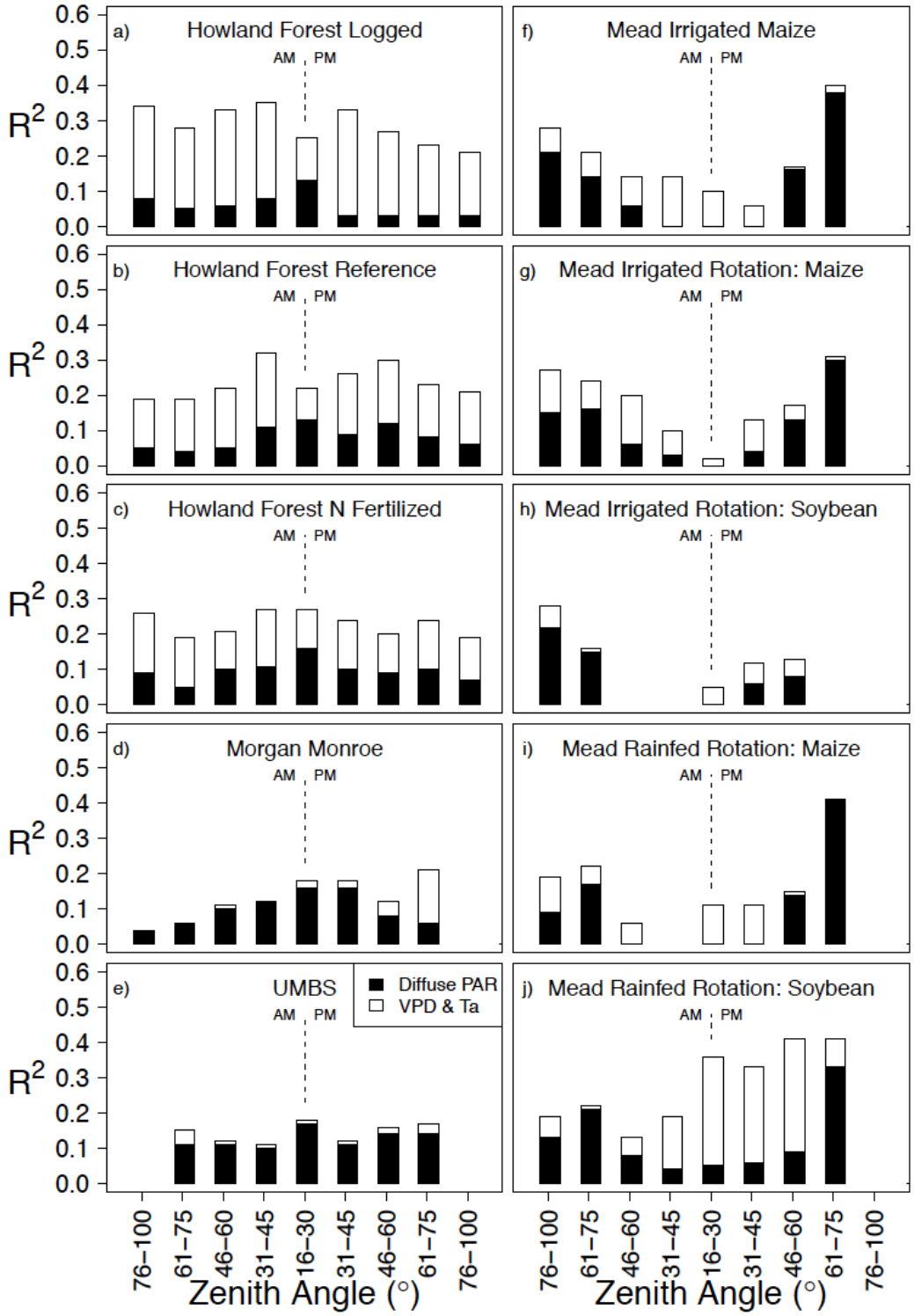

Fig 2: Proportions of variation in GPP_r explained by environmental variables. Solid bars represent R^2 values from simple linear regressions that include only the effect of diffuse PAR (Eq. 3). The total height of the bars (solid and white together) represents the R^2 from multiple linear regressions that include effects of air temperature (T_a) and vapor pressure deficit (VPD) with diffuse PAR (Eq. 4). Only R^2 values with $p < 6.02 \times 10^{-4}$ (Bonferroni-corrected critical value) are plotted. The minimum calculated zenith angle for these sites was ~16°.

3.2 Diffuse PAR cross-correlation with VPD and air temperature

Concomitant with changes in the partitioning of PAR into direct and diffuse streams, clouds and aerosols change surface VPD and air temperature. These two environmental factors influence stomatal conductance and photosynthesis, and thus affect rates of ecosystem GPP. When including the effects of these two variables on GPP_r with diffuse PAR (Eq. 4), the amount of variation in GPP_r explained increases up to an additional 31% during mornings and up to 32% during afternoons (Fig 2, white bars). This increase with VPD and air temperature is greatest across the most zenith angles at the Howland sites, where the multiple linear regression increases explanatory power of GPP_r by an additional 9-27% and 11-30% in the mornings and afternoons, respectively. VPD and air temperature also account for a relatively larger fraction of the variation of Mead Rainfed Rotation: Soybean GPP_r during the mid-day. Although we expected an increase in explanatory power with more variables in the regression, the increase in the explanation of GPP_r with the addition of these correlated environmental variables is small for the deciduous forests (Morgan Monroe and UMBS). This suggests that the effect of diffuse PAR at the deciduous forests is due to changes in light availability and not from indirect effects driven by the cross-correlation between diffuse PAR and other environmental conditions. Overall, the multiple linear regressions indicate that diffuse PAR is a significant predictor of GPP_r (except for the sites and zenith angle bins noted in Table 2). In addition, VPD and air temperature could not account for significant amounts of GPP_r variation under some conditions (Table 2).

Table 2: Parameter estimate values from relationships between GPP_r and diffuse PAR, vapor pressure deficit (VPD), and air temperature (T_a). All β_i estimate values (Eq. 4) have $p < 6.02 \times 10^{-4}$ (Bonferroni-corrected critical value), except for those designated as NS.

Site	β_i	Zenith Angle (°)								
		AM				PM				
		76-100	61-75	46-60	31-45	16-30	31-45	46-60	61-75	76-100
Howland Logged	Diffuse PAR	0.014	0.007	0.004	0.004	0.005	0.003	0.004	0.008	0.009
	VPD	-3.629	-2.627	-2.234	-3.847	-3.271	-3.205	-2.605	-2.339	-1.307
	T_a	0.183	0.343	0.427	0.546	0.352	0.495	0.383	0.296	0.172
Howland Reference	Diffuse PAR	0.010	0.005	0.004	0.005	0.005	0.005	0.008	0.010	0.011
	VPD	-2.004	NS	-1.914	-3.290	-2.728	-2.768	-2.309	-1.715	-1.208
	T_a	0.125	0.266	0.358	0.432	0.260	0.311	0.237	0.152	0.131
Howland N Fertilized	Diffuse PAR	0.014	0.007	0.006	0.005	0.006	0.006	0.007	0.012	0.014
	VPD	-2.625	NS	-1.876	-3.266	-3.204	-2.735	-2.052	-2.072	-1.330
	T_a	0.150	0.270	0.287	0.380	0.252	0.254	0.156	0.145	0.143
Morgan Monroe	Diffuse PAR	NS	0.010	0.011	0.010	0.008	0.009	0.008	0.008	NS
	VPD	NS	NS	NS	NS	-1.611	-1.734	-1.917	-2.479	NS
	T_a	NS	NS	NS	NS	NS	NS	NS	0.224	NS
UMBS	Diffuse PAR	NS	0.018	0.015	0.010	0.011	0.009	0.012	0.018	NS
	VPD	NS	4.218	3.078	NS	NS	NS	NS	-1.156	NS
	T_a	NS	NS	NS	-0.298	NS	NS	NS	NS	NS
Mead Irrigated Maize	Diffuse PAR	0.021	0.022	0.013	NS	NS	NS	0.024	0.050	NS
	VPD	NS	NS	NS	NS	-5.650	-3.061	NS	-1.252	NS
	T_a	0.304	0.445	0.811	1.315	1.215	0.660	NS	0.245	NS
Mead Irrigated Rotation: Maize	Diffuse PAR	0.019	0.021	0.012	0.011	NS	NS	0.027	0.042	NS
	VPD	NS	NS	NS	NS	NS	NS	NS	NS	NS
	T_a	0.332	NS	1.115	0.950	NS	1.135	NS	NS	NS
Mead Irrigated Rotation: Soybean	Diffuse PAR	0.017	0.015	NS	NS	NS	NS	0.011	NS	NS
	VPD	NS	NS	NS	NS	NS	NS	NS	NS	NS
	T_a	0.213	NS	NS	NS	0.598	0.534	NS	NS	NS
Mead Rainfed Rotation: Maize	Diffuse PAR	0.011	0.021	NS	NS	NS	NS	0.021	0.045	NS
	VPD	NS	NS	NS	NS	-6.365	-4.205	NS	NS	NS
	T_a	0.281	NS	NS	NS	NS	NS	NS	NS	NS
Mead Rainfed Rotation: Soybean	Diffuse PAR	0.014	0.021	NS	NS	NS	NS	NS	0.028	NS
	VPD	-3.148	NS	-5.123	-8.292	-8.021	-6.898	-5.035	-1.971	NS
	T_a	0.277	NS	NS	0.812	0.524	0.582	0.479	NS	NS

3.3 Magnitude of the effects of diffuse PAR on GPP_r

Howland Forest Reference, Morgan Monroe, and UMBS have not undergone any experimental manipulation (e.g., selective logging, N addition). At these sites, the sign of the significant parameter estimates indicate that in mornings and afternoons, GPP_r increased with diffuse PAR (Table 2). The predicted increases in GPP_r in the morning were calculated to be 0.004-0.010, 0.008-0.011, and 0.010-0.018 μmol CO_2 per μmol photons of diffuse PAR at Howland Forest Reference, Morgan Monroe, and UMBS, respectively (Fig. 3). In the afternoon, the increases in GPP_r were similar in magnitude, and ranged from 0.005-0.011, 0.008-0.009, and 0.009-0.018 μmol CO_2 per μmol photons of diffuse PAR at Howland Forest Reference, Morgan Monroe, and UMBS, respectively (Fig. 3).

The effect of diffuse PAR on rates of GPP_r varied among forest sites. UMBS had the largest increases in GPP_r with increases in diffuse PAR, and Howland Forest Reference had the smallest increases in GPP_r. In addition, the calculated increases in GPP_r with diffuse PAR appear to depend on zenith angle at two of the sites. At UMBS, the influence of diffuse PAR on GPP_r is greatest in the early morning and late afternoon (zenith angles 61-75°) and decreases at mid-day (zenith angles 16-45°). At Howland Forest Reference, the response to zenith angle differs and the influence of diffuse PAR on GPP_r generally increases as the day continues and is highest in the late afternoon (zenith angles 76-100°). However, at Morgan Monroe, the influence of diffuse PAR on GPP_r did not vary with zenith angle. When we compare across these ecosystems, deciduous forests (UMBS, Morgan Monroe) appear to differ from the mixed conifer forest, particularly in the morning, with differences diminishing in the afternoon.

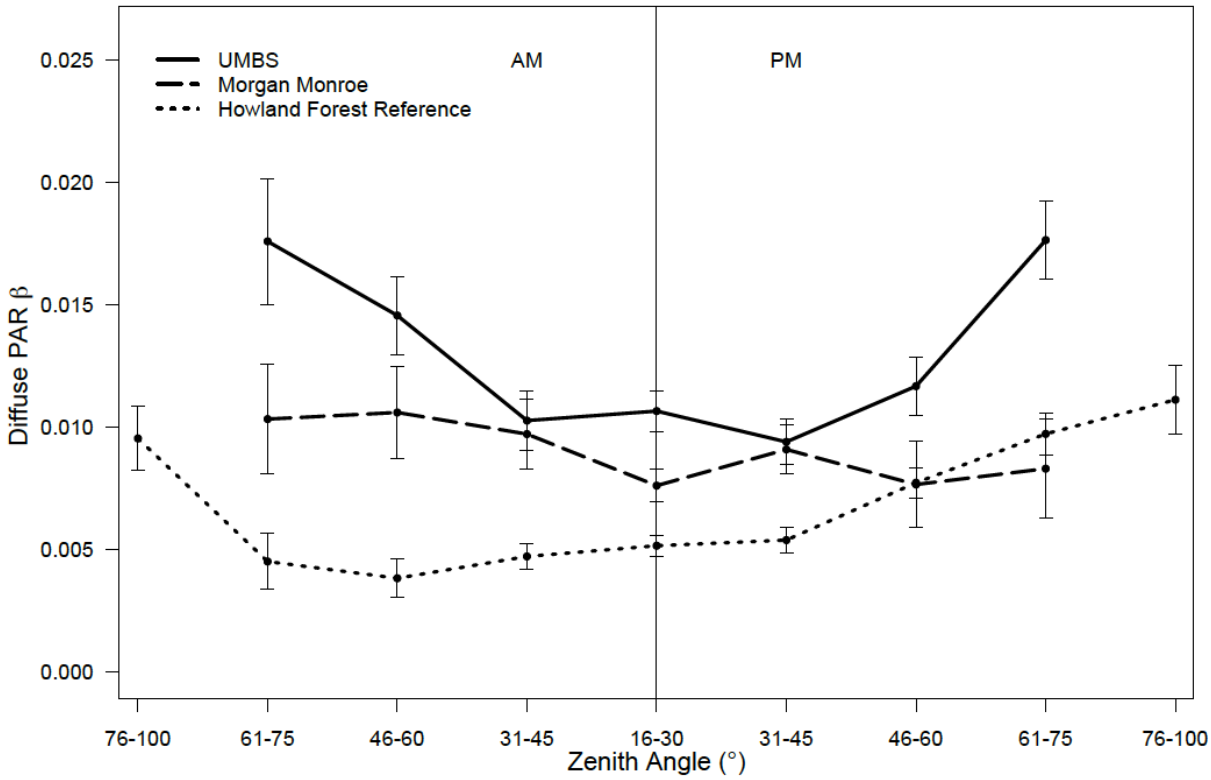

Fig 3. Diurnal patterns in diffuse PAR β estimates for unmanaged forests across zenith angles from a multiple linear regression that includes VPD and air temperature as covariates (Eq. 4). Error bars indicate one standard error. Only β estimates with $p < 6.02 \times 10^{-4}$ (Bonferroni-corrected critical value) are plotted.

298

299 At Howland Forest, one site underwent selective logging while a second site was
300 fertilized with 18 kg N/ha on a 21-hectare plot centered around the eddy covariance tower in five
301 to six applications per growing season from 2001-2005 (David Dail, personal communication,
302 2013). Analysis of data at these manipulated sites indicates that the magnitude of increase in
303 GPP_r with diffuse PAR was similar to that of the un-manipulated Howland forest (Fig. 4).
304 Differences among forest treatments are not apparent in the morning. In the afternoon, however,
305 we observe a trend where diffuse PAR leads to the biggest GPP_r increase in the forest fertilized
306 with N and the smallest change in GPP_r in the forest that has been selectively logged.

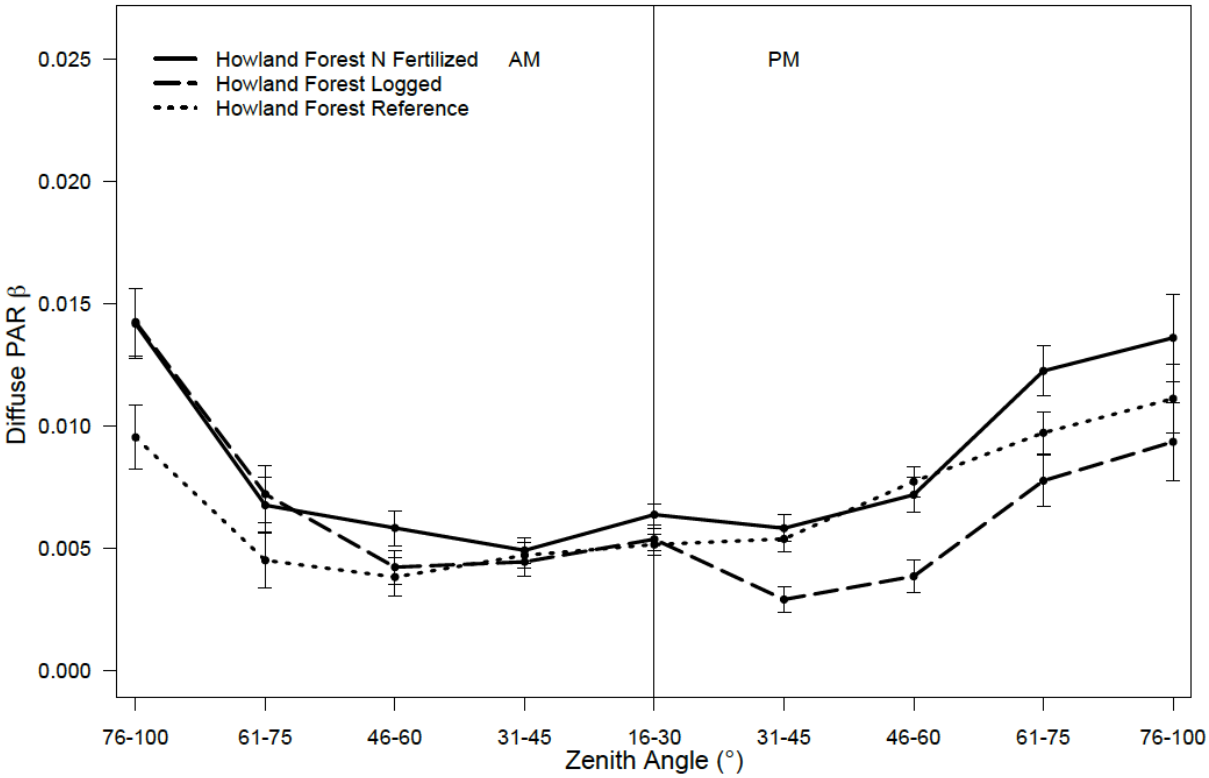

Fig 4: Diurnal patterns in diffuse PAR β estimate values for Howland Forest sites across zenith angles from a multiple linear regression that includes VPD and air temperature as covariates (Eq. 4). Error bars indicate one standard error. Only values with $p < 6.02 \times 10^{-4}$ (Bonferroni-corrected critical value) are plotted.

307

308 At the Mead Irrigated Rotation and Mead Rainfed Rotation sites, soybean and maize are
309 planted in different years, allowing us to examine variations in the effect of diffuse PAR on
310 GPP_r between crop types (Fig. 5). The increases in GPP_r for maize were calculated to be 0.011-
311 0.022 μmol CO_2 per μmol photons in the morning and 0.021-0.050 μmol CO_2 per μmol photons
312 in the afternoon. For soybean, the increases in GPP_r in the morning were 0.014-0.021 μmol CO_2
313 per μmol photons and in the afternoon were 0.011-0.028 μmol CO_2 per μmol photons. Diffuse
314 PAR led to increases in GPP_r at large zenith angles, but had no effect on GPP_r at small zenith
315 angles for both crop species (values are only plotted in Fig. 5 if they are significant). In addition,
316 we observed no difference in the magnitude of the effect of diffuse PAR on GPP_r between
317 soybean and maize in the morning. However, we did observe a greater effect of diffuse PAR on

318 GPP_r for maize than soybean in the afternoon for zenith angles 46-75°. Irrigation did not appear

319 to influence the magnitude of the diffuse PAR effect on GPP_r.

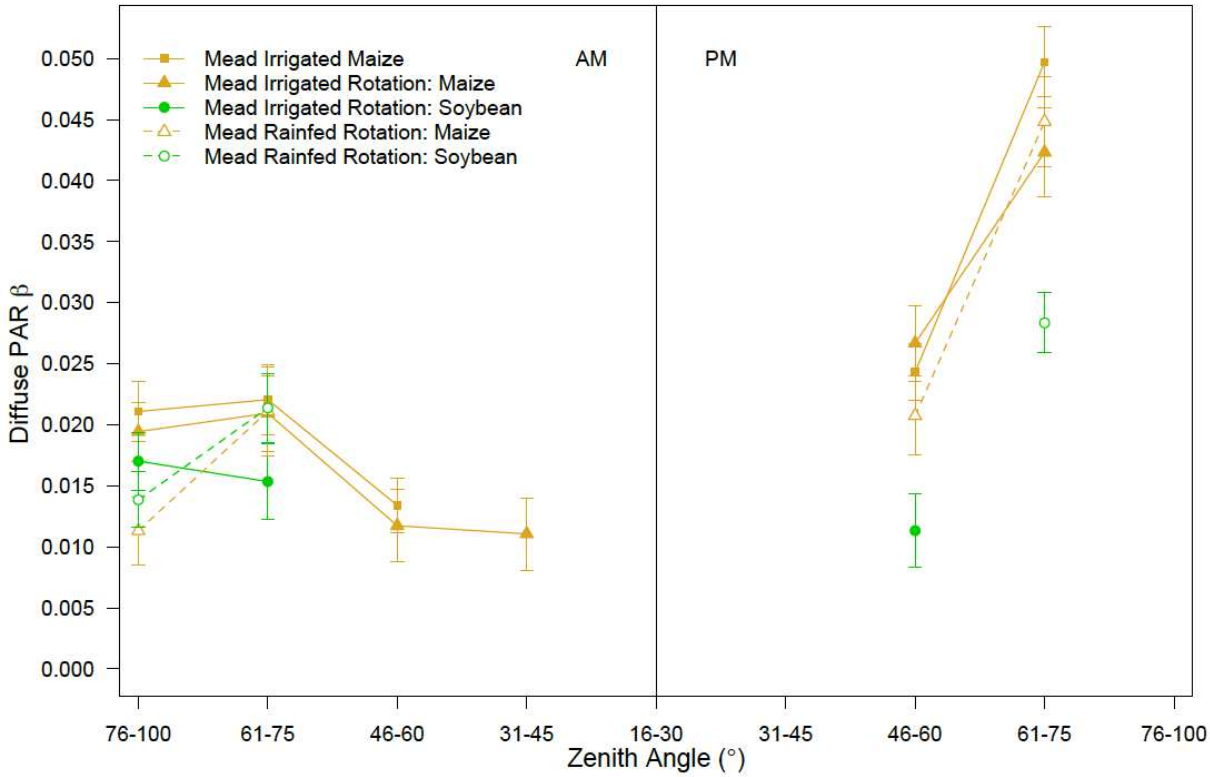

Fig 5: Diurnal patterns in diffuse PAR β estimate values for Mead crop sites across zenith angles from a multiple linear regression that includes VPD and air temperature as covariates (Eq. 4). Error bars indicate one standard error. Only β values with $p < 6.02 \times 10^{-4}$ (Bonferroni-corrected critical value) are plotted.

320

321 **4. Discussion**

322 Diffuse light influences Earth's climate by changing the amount and character of light

323 available for photosynthesis, and thus, indirectly controls atmospheric CO_2 (Mercado et al.,

324 2009). Depending on future anthropogenic emissions and their effects on atmospheric aerosols

325 and clouds, the influence of diffuse light on the terrestrial carbon sink may increase. A more

326 quantitative and mechanistic understanding of the link between diffuse light and land carbon

327 uptake in different ecosystems would allow us to model how changes in diffuse light influence

328 atmospheric and terrestrial carbon stocks, particularly as land-use change (e.g., deforestation,
329 afforestation, and conversion of natural systems to cropland) continues (Arora and Boer, 2010).
330 Past research has identified a positive correlation between diffuse light and ecosystem
331 carbon uptake. However, this result may be due to a cross-correlation with total light
332 availability, where diffuse light could more strongly influence photosynthesis when total light
333 levels are low on overcast days as compared to high light levels on clear days (Gu et al., 1999b;
334 Oliphant et al., 2011; Zhang et al., 2010). The method we use in this paper addresses this
335 confounding factor by removing the effect of direct light on ecosystem carbon uptake before
336 calculating the rate of additional carbon uptake from diffuse light. Importantly, we tested for this
337 potential independent effect using only direct field measurements of diffuse light, as opposed to
338 deriving diffuse light levels with radiation partitioning models that make assumptions about
339 aerosol and cloud conditions over terrestrial ecosystems. Our analysis of ten temperate
340 ecosystems indicates that diffuse PAR correlates positively with GPP_r and this relationship is
341 independent of direct PAR levels. Specifically, diffuse PAR independently explained up to 22%
342 of the variation in GPP_r in mornings and up to 41% of the variation in GPP_r in afternoons.
343 Prior research shows that morning and afternoon responses to diffuse light can differ for
344 the same zenith angles (Alton et al., 2005) and that in multiple ecosystems, rates of carbon
345 enhancement vary across zenith angles (Bai et al., 2012; Zhang et al., 2010). However, to our
346 knowledge, no other studies have investigated full diurnal patterns of diffuse light enhancement.
347 We accomplished this by separating data according to zenith angle and time of day. Our results
348 indicate that in forests, the proportion of variation in GPP_r explained by diffuse PAR (evaluated
349 through R^2) is greatest at mid-day, and decreases as the sun moves closer to the horizon. The
350 opposite pattern occurs at crop sites, where diffuse PAR did not predict GPP_r at small zenith

angles (mid-day), but did correlate with variation in GPP_r at larger zenith angles (morning and afternoon). When we examined the magnitude of increase in GPP_r in response to diffuse PAR (β_1), the greatest increases were at larger zenith angles in crop sites (0.028 - 0.050 μmol CO_2 per μmol photons at 61-75° in the afternoon). In forests, however, diffuse PAR had the strongest influence (R^2) on GPP_r at small zenith angles when the sun is overhead (mid-day), but the largest carbon enhancement rate (β_1) at larger zenith angles (early mornings and late afternoons) when the sun is closer to the horizon.

In addition, some sites show a trend in an asymmetrical diurnal cycle of diffuse light enhancement, most notably in the crop sites. Although increases in GPP_r with diffuse PAR at forest sites appear to be similar in magnitude throughout the day, some of the zenith angle bins differed between the morning and afternoon. For example, the largest difference in carbon enhancement rates from a morning zenith angle bin to the same bin in the afternoon were 0.005 μmol CO_2 per μmol photons for mixed conifer forests, 0.003 μmol CO_2 per μmol photons for deciduous forests, 0.017 μmol CO_2 per μmol photons for soy, and 0.028 μmol CO_2 per μmol photons for maize, though changes were usually within the standard error of the measurements. The response of GPP_r to diffuse light may differ in the morning and afternoon because environmental conditions influencing photosynthesis also vary during the day. For example, time lags between the effects of diurnal cycles of radiation and VPD on evapotranspiration (Zhang et al., 2014), stronger hydraulic stresses in the afternoon (Matheny et al., 2014), and morning and afternoon differences in leaf surface wetness that affect stomatal conductance (Misson et al., 2005) might explain the increased importance of diffuse light in the afternoon. These results can be used to evaluate ecosystem and global land surface models by testing if they capture the diurnal patterns we identified.

374 Our results indicate that there are ecosystem-specific responses of carbon uptake to
375 diffuse light. The observed differences between crops and forests are consistent with Niyogi et
376 al., 2004 who used measured diffuse shortwave data to show that a crop site with a corn and
377 soybean rotation was more sensitive to increases in aerosol-produced diffuse light than broadleaf
378 and mixed conifer forests. Previous studies have hypothesized that differences in canopy
379 structure among forests, grasslands, and croplands are responsible for differential responses of
380 these ecosystems to diffuse light (Gu et al., 1999a; Niyogi et al., 2004; Oliphant et al., 2011).
381 However, they have not reported site-level canopy architectural measurements to test this
382 potential modifier of land carbon uptake because they are difficult to collect and describe.
383 There are several hypotheses explaining why canopy structure may modify the effect of
384 diffuse light on ecosystem carbon uptake. Canopy gaps, which interact with the angle of
385 incident light, may influence how much light is distributed vertically through a canopy
386 (Hutchison et al., 1980). For example, on clear days in a 30-m tall tulip poplar forest, the
387 amount of radiation reaching the mid- and lower-parts of the canopy is lowest at large zenith
388 angles (Hutchison et al., 1980). The authors attributed this to the low level of total radiation and
389 reduced canopy gaps when the sun is near the horizon. Our analysis of UMBS gap fraction data
390 derived from LAI-2000 measurements shows that as gap fraction decreases, carbon uptake with
391 diffuse light increases (Fig. 6). Because gap fraction here is the ratio of below-canopy PAR to
392 above-canopy PAR, this indicates greater light extinction at larger zenith angles. Greater light
393 extinction in the canopy may increase light scattering, which could expose more leaves to diffuse
394 light. Thus, the response of GPP to diffuse light may be greater at larger zenith angles because
395 of more complete canopy participation in photosynthesis. However, more gap fraction data and
396 canopy light profiles from across sites and collected with uniform methods are needed to test this

idea, particularly in crop ecosystems. This would allow us to identify why crops and forests respond differently to diffuse PAR.

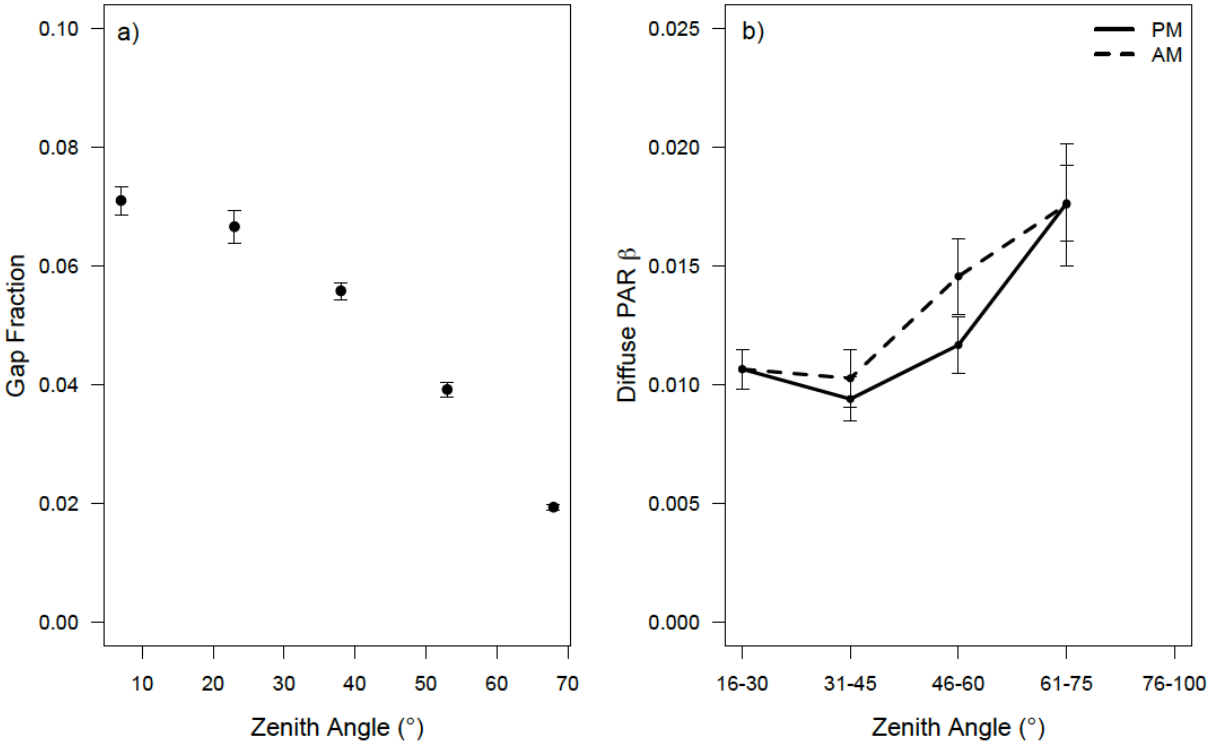

Fig. 6. The relationship at UMBS (data from 2007-2011) between a) gap fraction and zenith angle and b) diffuse PAR β (carbon enhancement rate) and zenith angles (same data as shown in Fig. 3). Error bars indicate one standard error.

Second, the distribution of photosynthetic tissues within a canopy depends on the plant community at each site and may contribute to observed differences between crops and forests. Forests have more stratified layers of vegetation and are much taller than crops. This means that leaf area index (LAI) in a forest is distributed over a larger volume than in crop sites. When the sun is overhead, forest canopies shade leaves at lower layers and diffuse light has a greater potential of reaching leaves near the bottom of the forest canopy as compared to direct light. Thus, the opportunity for diffuse light to reach more leaves in the canopy is greater when the sun is overhead (larger R^2). This explanation is supported by a study in a Norway spruce forest,

408 which showed that needles deeper in the canopy contribute more to overall net ecosystem
409 production on cloudy days than on sunny days (Urban et al., 2012). However, the relative
410 increases in GPP (β_1) may be smaller than those at crop sites because forest canopies are denser,
411 which increases self-shading. On the other hand, crops are planted to minimize self-shading
412 when the sun is overhead. In addition, β_1 may be higher at crop sites than at forests because
413 multi-directional diffuse light at large zenith angles may reach deeper into crop canopies more
414 effectively than direct light and increase light availability for crop stems, which are more
415 photosynthetic than tree trunks.

416 Modeling studies have shown that species-dependent canopy characteristics, such as leaf
417 clumping, LAI, and leaf inclination angle can affect the influence of diffuse PAR on carbon
418 processing in ecosystems (Alton, 2008; Gu et al., 2002; Knohl and Baldocchi, 2008). This could
419 be due to the penumbral effect, which occurs when the position and types of leaves (e.g.,
420 broadleaf and conifer) alter the amount and distribution of light to lower-level leaves (Denholm,
421 1981; Way and Pearcy, 2012). Although the arrangement of leaves in tall canopies with small
422 leaves (e.g., forests) can increase shading of lower canopy leaves, it also increases the probability
423 that leaves and branches scatter light, resulting in more distribution of light in the canopy.
424 However, in shorter canopies with larger leaves (e.g., maize), there is less plant material that can
425 scatter light and these sites may be more dependent on incident diffuse light. This may explain
426 the higher carbon enhancement rates observed at crop sites compared to forests.

427 A few studies have measured how the distribution of light through plant canopies
428 changes under diffuse light, but they are limited in their ability to test the influence of canopy
429 structure on carbon enhancement from diffuse light because they have been conducted in a single
430 ecosystem (Urban et al., 2012; Williams et al., 2014). Because site-level measurements of

canopy structure are difficult to obtain, support for the mechanisms through which specific characteristics of canopy structure (e.g., leaf area distribution, leaf clumping) change ecosystem carbon uptake under diffuse light conditions has thus far depended on model assumptions (Alton et al., 2007; Knohl and Baldocchi, 2008). To test whether canopy structural differences in height, canopy gaps, or leaf distribution within a canopy facilitate a diffuse light enhancement, a uniform method of collecting canopy structural data is needed. Methods are available for capturing some of this information, including light detection and ranging (LIDAR) remote sensing (Hardiman et al., 2013). However, no standardized method of collecting data has been applied among sites to allow for inter-site comparisons of canopy structure. Future research should consider collecting data on canopy gaps, leaf distribution, and vertical light distribution to provide datasets that can be used to test whether gaps or leaf distribution within a canopy lead to an enhanced carbon uptake because of increased light distribution. Without this mechanistic connection, modelers cannot determine whether this missing biosphere-atmosphere connection results in a significant under- or over-prediction of the future terrestrial carbon sink. As scientists collect these canopy structural data, we suggest making these data publically available so they can be used to better interpret patterns seen using eddy covariance data.

We also observed differences in diffuse light effects among sites described as the same forest type (e.g., Morgan Monroe and UMBS). This argues for the consideration of site-specific responses to diffuse light because plant community composition of individual forest types (or ecosystems) determine unique canopy structures that can drive how strongly canopy gaps, leaf distribution, and penumbral qualities influence the effect of diffuse light on ecosystem carbon uptake. In particular, there were differences in afternoon carbon enhancement rates between the fertilized and formerly logged Howland Forest sites, which only differ in disturbance activity.

454 Differences in nutrient availability for plants may explain why the N fertilized site correlated
455 more strongly with diffuse light than the logged site. After two years of fertilization, foliage was
456 one of the most N-enriched ecosystem pools (Dail et al., 2009). Increased soil N availability
457 could lead to an increase in leaf N, which correlates with higher concentrations of RuBisCO and
458 chlorophyll (Evans, 1989), implying an interaction between diffuse light and nutrient levels.
459 The effect of diffuse light on carbon uptake between maize and soybean also differed.
460 This may be due to species differences in canopy structure as discussed above, but could also be
461 due to the different photosynthetic pathways soy (C_3) and maize (C_4) use. Maize had a greater
462 increase in carbon uptake with diffuse light than soy did, potentially because C_4 plants have a
463 higher light saturation point (Greenwald et al., 2006). Because maize would be farther away
464 from light saturation than soy, an increase in diffuse light (after accounting for cross-correlation
465 with direct light) would bring maize closer to light saturation and thus, increase photosynthesis.
466 In addition, C_4 plants are better adapted to warmer environments, which may cause
467 environmental conditions, such as temperature and water availability, to change crop responses
468 to diffuse light.
469 Finally, our results show that other environmental drivers that co-vary with diffuse PAR
470 also contribute to GPP_r at some sites. In mixed conifer forests (e.g., the Howland sites), VPD,
471 air temperature, and diffuse PAR together account for substantially more variation in GPP_r than
472 diffuse PAR itself does, implying a lesser role for radiation and a larger one for conditions that
473 improve stomatal conductance under cloudy conditions at mixed conifer forests. In contrast,
474 VPD and air temperature, within the ranges of values characteristic of measurement periods at
475 the sites studied here, appear to have small effects on GPP_r in the broadleaf forests. This implies
476 that the diffuse PAR effect at the broadleaf forests is due to the effect of scattered light itself. At

477 the mixed conifer forests, the peak growing season temperature ranges from 16.5-17.6°C while
478 the temperature is 21.2-24.3°C in the broadleaf forests. Comparing these site temperatures to the
479 optimum temperature range of temperate deciduous trees (20-25°C) and evergreen coniferous
480 trees (10-25°C), broadleaf forests are closer to their optimum temperature range (Larcher, 2003).
481 Considering that photosynthesis varies non-linearly with temperature, the same per unit change
482 in temperature for a cooler site will lead to greater changes in GPP than in a warmer site.
483 Increases in VPD in water-limited situations, on the other hand, should cause photosynthesis to
484 drop because stomata will close to conserve water. However, VPD is actually lower in the
485 mixed forests than in the deciduous broadleaf forests, implying that air temperature is a stronger
486 driver of GPP than is VPD under our study's field conditions.

487 **5. Conclusions**

488 Field measurements show that diffuse PAR accounts for a substantial amount of variation
489 in GPP once the quantity of direct PAR is removed. The observed changes in the diffuse PAR
490 effect on GPP_r vary across zenith angles, ecosystem types, and plant functional groups,
491 highlighting additional ways that ecosystem structural characteristics and the diurnal cycle
492 influence ecosystem carbon cycling. In addition, observed site-level variation suggests that
493 grouping forests together in regional or global models as the same plant functional type, without
494 considering species composition or canopy structure, may lead to inaccuracies in assessing the
495 impacts of radiation partitioning on modeled surface carbon fluxes.

496 To robustly extend these results, direct measurements of diffuse PAR and ecosystem flux
497 data are needed from a wider range of ecosystems. Furthermore, research that can evaluate
498 mechanisms (e.g, canopy gaps, leaf distribution, and species-specific characteristics) driving
499 terrestrial carbon enhancement under diffuse light will remain stagnant without consistent field

measurements of canopy structure at sites with diffuse light and eddy covariance measurements. The incorporation of standard methods for measuring canopy structure and within-canopy light distribution and the availability of these data in common formats from across networks of eddy covariance towers (e.g., AmeriFlux, NEON) would enable the development of better predictive models of carbon exchange in relation to direct and diffuse solar radiation.

The interactions between diffuse light and ecosystem productivity may be of increasing importance as the community composition of our terrestrial ecosystems continues to change because of human land use change, natural ecological succession, and climate change. Thus, a more refined understanding of how diffuse PAR modifies atmosphere-land carbon cycling and subsequent representations of this relationship in models will likely advance our understanding of how human management of ecosystems will influence the land carbon sink as well as improve future calculations of atmospheric CO_2 concentrations for global climate projections.

Acknowledgments

We thank the FLUXNET community for their dedicated efforts in collecting and providing quality-controlled eddy covariance data for ecosystem research. We also thank the University of Michigan Center for Statistical Consultation and Research (Dr. Corey Powell and Dr. Kerby Shedden) for input on statistical techniques, Dr. Christoph Vogel for providing updated PAR data for UMBS, and Alex Fotis for early discussions and data organization for this paper. Support for SJC was provided in part by the University of Michigan Graham Sustainability Institute. Funding for data collection at UMBS was provided by the National Science Foundation grant DEB-0911461, the U.S. Department of Energy's (DOE) Office of Science Biological and Environmental Research (BER) project DE-SC0006708 and AmeriFlux National Core Flux Site award through Lawrence Berkeley National Laboratory contract

#7096915, and National Oceanic and Atmospheric Administration grant NA11OAR4310190. Research at the Howland Forest is supported by the DOE's Office of Science BER. The Mead US-Ne1, US-Ne2, and US-Ne3 AmeriFlux sites were supported by the DOE Office of Science (BER; Grant Nos. DE-FG03-00ER62996, DE-FG02-03ER63639, and DE-EE0003149), DOE-EPSCoR (Grant No. DE-FG02-00ER45827), and NASA NACP (Grant No. NNX08AI75G). The Morgan Monroe team thanks the Indiana Department of Natural Resources for supporting and hosting the UM-MMS AmeriFlux site, and the U.S. DOE for funding operations through the Terrestrial Ecosystem Science program and the AmeriFlux Management Project.

Appendices

Appendix 1: Values of α and γ predicted by best-fit rectangular hyperbolas describing the response of GPP to direct PAR. The α represents the quantum yield and γ represents the maximum GPP value. All α and γ values listed have $p < 6.02 \times 10^{-4}$ (Bonferroni-corrected critical value), except for those in italics, which have $p < 0.01$ and those in **bold**, which were not significant because $p > 0.05$. NS indicates we were unable to fit a light response curve.

Site		Zenith Angle (°)								
		AM					PM			
		76-100	61-75	46-60	31-45	16-30	31-45	46-60	61-75	76-100
Howland Forest Logged	α	1.16	2.64	2.82	2.74	3.41	2.58	2.61	2.07	1.10
	γ	7.41	11.84	14.67	16.52	18.12	14.57	12.93	10.04	6.39
	R^2	0.39	0.37	0.34	0.26	0.27	0.29	0.33	0.37	0.39
Howland Forest Reference	α	1.28	2.15	2.41	2.30	2.27	2.21	2.13	1.89	1.91
	γ	4.74	9.89	14.15	16.16	17.15	13.93	11.64	8.35	4.53
	R^2	0.23	0.34	0.34	0.34	0.35	0.33	0.38	0.39	0.21
Howland Forest N Fertilized	α	1.81	2.85	2.93	2.38	2.82	3.28	3.79	2.85	2.01
	γ	5.27	10.32	14.20	17.14	17.77	14.71	12.05	8.82	5.04
	R^2	0.25	0.32	0.35	0.37	0.29	0.24	0.21	0.27	0.18
Morgan Monroe	α	*2.01*	1.43	1.59	1.50	2.03	1.99	2.09	2.58	NS
	γ	4.66	12.39	19.83	25.72	27.29	22.99	16.78	10.31	NS
	R^2	0.06	0.13	0.23	0.32	0.29	0.31	0.22	0.25	NS
UMBS	α	1.05	*3.57*	4.06	3.08	2.99	3.96	1.59	1.43	3.00
	γ	6.07	12.36	20.38	25.32	27.10	23.78	19.17	13.25	6.94
	R^2	0.28	0.09	0.11	0.15	0.12	0.14	0.24	0.34	0.21
Mead Irrigated Maize	α	0.73	3.95	4.49	3.35	2.98	3.51	1.61	2.07	NS
	γ	16.11	30.91	48.21	59.92	64.10	49.94	35.94	17.71	NS
	R^2	0.49	0.21	0.22	0.31	0.23	0.29	0.20	0.13	NS
Mead Irrigated Rotation: Maize	α	0.40	1.65	2.60	2.48	3.30	1.20	1.29	0.64	NS
	γ	17.61	32.62	48.64	58.70	65.20	50.15	38.13	21.68	NS
	R^2	0.51	0.47	0.43	0.38	0.42	0.41	0.36	0.38	NS
Mead Irrigated Rotation: Soybean	α	0.59	2.24	6.35	5.37	5.29	6.48	*3.51*	NS	NS
	γ	12.20	23.63	31.62	37.67	36.42	31.74	23.52	NS	NS
	R^2	0.59	0.45	0.27	0.29	0.27	0.21	0.23	NS	NS
Mead Rainfed Rotation: Maize	α	0.54	3.39	4.67	4.21	3.78	3.23	2.31	0.94	NS
	γ	17.47	31.51	44.79	55.53	56.19	46.60	33.49	18.65	NS
	R^2	0.66	0.53	0.48	0.53	0.37	0.39	0.29	0.44	NS
Mead Rainfed Rotation: Soybean	α	0.75	4.69	*16.67*	*9.43*	**15.38**	**31.88**	**5.89**	1.35	NS
	γ	13.11	23.44	29.27	34.98	30.74	29.40	20.29	13.47	NS
	R^2	0.53	0.16	0.08	0.05	0.01	0.00	0.04	0.18	NS

References

Alton, P.B., 2008. Reduced carbon sequestration in terrestrial ecosystems under overcast skies compared to clear skies. Agricultural and Forest Meteorology, 148(10): 1641-1653.

Alton, P.B., North, P., Kaduk, J. and Los, S., 2005. Radiative transfer modeling of direct and diffuse sunlight in a Siberian pine forest. Journal of Geophysical Research: Atmospheres, 110(D23): D23209.

Alton, P.B., North, P.R. and Los, S.O., 2007. The impact of diffuse sunlight on canopy light-use efficiency, gross photosynthetic product and net ecosystem exchange in three forest biomes. Global Change Biology, 13(4): 776-787.

Arora, V.K. and Boer, G.J., 2010. Uncertainties in the 20th century carbon budget associated with land use change. Global Change Biology, 16(12): 3327-3348.

Bai, Y., Wang, J., Zhang, B., Zhang, Z. and Liang, J., 2012. Comparing the impact of cloudiness on carbon dioxide exchange in a grassland and a maize cropland in northwestern China. Ecological Research, 27(3): 615-623.

Baldocchi, D.D., 2003. Assessing the eddy covariance technique for evaluating carbon dioxide exchange rates of ecosystems: past, present and future. Global Change Biology, 9(4): 479-492.

Bonan, G.B., Oleson, K.W., Fisher, R.A., Lasslop, G. and Reichstein, M., 2012. Reconciling leaf physiological traits and canopy flux data: Use of the TRY and FLUXNET databases in the Community Land Model version 4. Journal of Geophysical Research: Biogeosciences, 117(G2): G02026.

Butt, N. et al., 2010. Diffuse radiation and cloud fraction relationships in two contrasting Amazonian rainforest sites. Agricultural and Forest Meteorology, 150(3): 361-368.

Campbell, G.S. and Norman, J.M., 1998. An introduction to environmental biophysics. An introduction to environmental biophysics.(Ed. 2).

Curtis, P.S. et al., 2002. Biometric and eddy-covariance based estimates of annual carbon storage in five eastern North American deciduous forests. Agricultural and Forest Meteorology, 113(1-4): 3-19.

Dai, Y., Dickinson, R.E. and Wang, Y.-P., 2004. A two-big-leaf model for canopy temperature, photosynthesis, and stomatal conductance. Journal of Climate, 17(12).

Dail, D.B. et al., 2009. Distribution of nitrogen-15 tracers applied to the canopy of a mature spruce-hemlock stand, Howland, Maine, USA. Oecologia, 160(3): 589-599.

Davin, E.L. and Seneviratne, S.I., 2012. Role of land surface processes and diffuse/direct radiation partitioning in simulating the European climate. Biogeosciences, 9(5): 1695-1707.

Dengel, S. and Grace, J., 2010. Carbon dioxide exchange and canopy conductance of two coniferous forests under various sky conditions. Oecologia, 164(3): 797-808.

Denholm, J.V., 1981. THE INFLUENCE OF PENUMBRA ON CANOPY PHOTOSYNTHESIS .1. THEORETICAL CONSIDERATIONS. Agricultural Meteorology, 25(3): 145-166.

Dragoni, D. et al., 2011. Evidence of increased net ecosystem productivity associated with a longer vegetated season in a deciduous forest in south-central Indiana, USA. Global Change Biology, 17(2): 886-897.

Evans, J., 1989. Photosynthesis and nitrogen relationships in leaves of C3 plants. Oecologia, 78(1): 9-19.

586 Garrity, S.R. et al., 2011. A comparison of multiple phenology data sources for estimating
587 seasonal transitions in deciduous forest carbon exchange. Agricultural and Forest
588 Meteorology, 151(12): 1741-1752.
589 Gough, C.M. et al., 2013. Sustained carbon uptake and storage following moderate disturbance
590 in a Great Lakes forest. Ecological Applications, 23(5): 1202-1215.
591 Greenwald, R. et al., 2006. The influence of aerosols on crop production: A study using the
592 CERES crop model. Agricultural Systems, 89(2–3): 390-413.
593 Gu, L. et al., 2002. Advantages of diffuse radiation for terrestrial ecosystem productivity. Journal
594 of Geophysical Research: Atmospheres, 107(D6): ACL 2-1-ACL 2-23.
595 Gu, L. et al., 2003. Response of a Deciduous Forest to the Mount Pinatubo Eruption: Enhanced
596 Photosynthesis. Science, 299(5615): 2035-2038.
597 Gu, L., Fuentes, J.D., Shugart, H.H., Staebler, R.M. and Black, T.A., 1999a. Responses of net
598 ecosystem exchanges of carbon dioxide to changes in cloudiness: Results from two North
599 American deciduous forests. Journal of Geophysical Research: Atmospheres, 104(D24):
600 31421-31434.
601 Gu, L., Fuentes, J.D., Shugart, H.H., Staebler, R.M. and Black, T.A., 1999b. Responses of net
602 ecosystem exchanges of carbon dioxide to changes in cloudiness: Results from two North
603 American deciduous forests. J. Geophys. Res., 104(D24): 31421-31434.
604 Hardiman, B.S. et al., 2013. Maintaining high rates of carbon storage in old forests: A
605 mechanism linking canopy structure to forest function. Forest Ecology and Management,
606 298(0): 111-119.
607 Hollinger, D.Y. et al., 2004. Spatial and temporal variability in forest–atmosphere CO2
608 exchange. Global Change Biology, 10(10): 1689-1706.
609 Hollinger, D.Y. et al., 1994. Carbon Dioxide Exchange between an Undisturbed Old-Growth
610 Temperate Forest and the Atmosphere. Ecology, 75(1): 134-150.
611 Hutchison, B.A., Matt, D.R. and McMillen, R.T., 1980. Effects of sky brightness distribution
612 upon penetration of diffuse radiation through canopy gaps in a deciduous forest.
613 Agricultural Meteorology, 22(2): 137-147.
614 Jenkins, J.P. et al., 2007. Refining light-use efficiency calculations for a deciduous forest canopy
615 using simultaneous tower-based carbon flux and radiometric measurements. Agricultural
616 and Forest Meteorology, 143(1-2): 64-79.
617 Knohl, A. and Baldocchi, D.D., 2008. Effects of diffuse radiation on canopy gas exchange
618 processes in a forest ecosystem. J. Geophys. Res., 113(G2): G02023.
619 Larcher, W., 2003. Physiolgical Plant Ecology. Springer, Berlin.
620 Law, B.E. et al., 2002. Environmental controls over carbon dioxide and water vapor exchange of
621 terrestrial vegetation. Agricultural and Forest Meteorology, 113(1–4): 97-120.
622 Le Quéré, C. et al., 2013. Global carbon budget 2013. Earth Syst. Sci. Data Discuss., 6(2): 689-
623 760.
624 Matheny, A.M. et al., 2014. Characterizing the diurnal patterns of errors in the prediction of
625 evapotranspiration by several land-surface models: An NACP analysis. Journal of
626 Geophysical Research: Biogeosciences, 119(7): 2014JG002623.
627 Matsui, T., Beltrán-Przekurat, A., Niyogi, D., Pielke, R.A., Sr. and Coughenour, M., 2008.
628 Aerosol light scattering effect on terrestrial plant productivity and energy fluxes over the
629 eastern United States. J. Geophys. Res., 113(D14): D14S14.
630 Mercado, L.M. et al., 2009. Impact of changes in diffuse radiation on the global land carbon
631 sink. Nature, 458(7241): 1014-U87.

Min, Q. and Wang, S., 2008. Clouds modulate terrestrial carbon uptake in a midlatitude hardwood forest. Geophys. Res. Lett., 35(2): L02406.
Misson, L., Lunden, M., McKay, M. and Goldstein, A.H., 2005. Atmospheric aerosol light scattering and surface wetness influence the diurnal pattern of net ecosystem exchange in a semi-arid ponderosa pine plantation. Agricultural and Forest Meteorology, 129(1–2): 69-83.
Niyogi, D. et al., 2004. Direct observations of the effects of aerosol loading on net ecosystem CO2 exchanges over different landscapes. Geophysical Research Letters, 31(20).
Oliphant, A.J. et al., 2011. The role of sky conditions on gross primary production in a mixed deciduous forest. Agricultural and Forest Meteorology, 151(7): 781-791.
R Development Core Team, 2012. R: A language and environment for statistical computing. R Foundation for Statistical Computing, Vienna, Austria.
Richardson, A.D. et al., 2013. Climate change, phenology, and phenological control of vegetation feedbacks to the climate system. Agricultural and Forest Meteorology, 169(0): 156-173.
Rocha, A.V., Su, H.-B., Vogel, C.S., Schmid, H.P. and Curtis, P.S., 2004. Photosynthetic and Water Use Efficiency Responses to Diffuse Radiation by an Aspen-Dominated Northern Hardwood Forest. Forest Science, 50(6): 793-801.
Ruimy, A., Jarvis, P.G., Baldocchi, D.D. and Saugier, B., 1995. CO2 Fluxes over Plant Canopies and Solar Radiation: A Review. In: M. Begon and A.H. Fitter (Editors), Advances in Ecological Research. Academic Press, pp. 1-68.
Sarmiento, J.L. et al., 2010. Trends and regional distributions of land and ocean carbon sinks. Biogeosciences, 7(8): 2351-2367.
Scott, N.A. et al., 2004. Changes in Carbon Storage and Net Carbon Exchange One Year After an Initial Shelterwood Harvest at Howland Forest, ME. Environmental Management, 33(1): S9-S22.
Steiner, A.L. and Chameides, W.L., 2005. Aerosol-induced thermal effects increase modelled terrestrial photosynthesis and transpiration. Tellus B, 57(5): 404-411.
Urban, O. et al., 2007. Ecophysiological controls over the net ecosystem exchange of mountain spruce stand. Comparison of the response in direct vs. diffuse solar radiation. Global Change Biology, 13(1): 157-168.
Urban, O. et al., 2012. Impact of clear and cloudy sky conditions on the vertical distribution of photosynthetic CO2 uptake within a spruce canopy. Functional Ecology, 26(1): 46-55.
Verma, S.B. et al., 2005. Annual carbon dioxide exchange in irrigated and rainfed maize-based agroecosystems. Agricultural and Forest Meteorology, 131(1-2): 77-96.
Wang, K., Dickinson, R.E. and Liang, S., 2008. Observational evidence on the effects of clouds and aerosols on net ecosystem exchange and evapotranspiration. Geophys. Res. Lett., 35(10): L10401.
Way, D.A. and Pearcy, R.W., 2012. Sunflecks in trees and forests: from photosynthetic physiology to global change biology. Tree physiology, 32(9): 1066-1081.
Williams, M., Rastetter, E.B., Van der Pol, L. and Shaver, G.R., 2014. Arctic canopy photosynthetic efficiency enhanced under diffuse light, linked to a reduction in the fraction of the canopy in deep shade. New Phytologist, 202(4): 1267-1276.
Yan, H. et al., 2012. Global estimation of evapotranspiration using a leaf area index-based surface energy and water balance model. Remote Sensing of Environment, 124: 581-595.

Zhang, M. et al., 2011. Effects of cloudiness change on net ecosystem exchange, light use efficiency, and water use efficiency in typical ecosystems of China. Agricultural and Forest Meteorology, 151(7): 803-816.
Zhang, Q., Manzoni, S., Katul, G., Porporato, A. and Yang, D., 2014. The hysteretic evapotranspiration—Vapor pressure deficit relation. Journal of Geophysical Research: Biogeosciences, 119(2): 2013JG002484.
Zhang, Y., Wen, X.Y. and Jang, C.J., 2010. Simulating chemistry–aerosol–cloud–radiation–climate feedbacks over the continental U.S. using the online-coupled Weather Research Forecasting Model with chemistry (WRF/Chem). Atmospheric Environment, 44(29): 3568-3582.